Supramolecular Chemistry
Publication details, including instructions for authors and subscription information:
http://www.informaworld.com/smpp/title~content=t713649759

Preparation, Thermal Behaviour and Solid-state Structures of Inclusion Complexes of Permethylated-β-cyclodextrin with the Garlic-derived Antithrombotics (*E*)- and (*Z*)-Ajoene

Mino R. Caira[a]; Roger Hunter[a]; Susan A. Bourne[a]; Vincent J. Smith[a]
[a] Department of Chemistry, University of Cape Town, Rondebosch, South Africa

To cite this Article Caira, Mino R. , Hunter, Roger , Bourne, Susan A. and Smith, Vincent J.(2004) 'Preparation, Thermal Behaviour and Solid-state Structures of Inclusion Complexes of Permethylated-β-cyclodextrin with the Garlic-derived Antithrombotics (*E*)- and (*Z*)-Ajoene', Supramolecular Chemistry, 16: 6, 395 — 403
To link to this Article: DOI: 10.1080/10610270412331285996
URL: http://dx.doi.org/10.1080/10610270412331285996

Supramolecular Chemistry, September 2004, Vol. 16 (6), pp. 395–403

Taylor & Francis
Taylor & Francis Group

Preparation, Thermal Behaviour and Solid-state Structures of Inclusion Complexes of Permethylated-β-cyclodextrin with the Garlic-derived Antithrombotics (*E*)- and (*Z*)-Ajoene

MINO R. CAIRA*, ROGER HUNTER, SUSAN A. BOURNE and VINCENT J. SMITH

Department of Chemistry, University of Cape Town, Rondebosch 7701, South Africa

Received (in Southampton, UK) 30 January 2004; Accepted 11 March 2004

The *E* and *Z* isomers of the antithrombotic ajoene (4,5,9-trithiadodeca-1,6,11-triene 9-oxide), components of garlic (*Allium Sativa*, L.), were complexed with heptakis(2,3,6-tri-*O*-methyl)-β-cyclodextrin (TRIMEB) to yield solid inclusion compounds with the compositions TRIMEB·(*E*)-ajoene·0.5H_2O (1) and TRIMEB·(*Z*)-ajoene (2). These species were investigated by thermal analysis techniques (HSM, TGA, DSC), powder X-ray diffraction (PXRD) and single-crystal X-ray diffraction at 173 K. Thermal analysis of 1 revealed dehydration followed by melting at 143.8°C, and only melting at 140.5°C for 2. The complexes yielded different PXRD traces, indicating crystallization in different arrangements. Single-crystal X-ray methods revealed the space groups $P2_1$ (1) and $P2_12_12_1$ (2) and the simultaneous presence of the guest stereoisomers in both complexes. Refinement of guest site-occupancies showed that each complex crystal consists of a mixture of diastereomers in 1:1 molar ratio. The different crystal packing arrangements for 1 and 2 are induced by the distinctly different modes of inclusion of the *E* and *Z* isomers.

Keywords: Permethylated-β-cyclodextrin; Thermal analysis; X-ray structures; Ajoene

INTRODUCTION

Pharmacologically active principles contained in garlic (*Allium Sativa*, L.), or derived from its constituents, have been investigated extensively during the past twenty years because of their established beneficial effects on human health [1,2]. Among the organosulfur compounds identified in garlic extracts, ajoene (4,5,9-trithiadodeca-1,6,11-triene 9-oxide) has enjoyed increasing attention in view of its remarkably wide range of activities, which includes antithrombotic [3], antimicrobial [4], antifungal [5], cytostatic and cytotoxic [6], hypocholesterolemic [7], antidiabetic [8], immunosuppressive and antineoplastic [9], anti-HIV [10] and other effects. Its isolation and *in vitro* inhibition of human platelet aggregation were reported in 1983 [3]. Spectroscopic and chemical studies by Block *et al.* [11,12] revealed that when allicin (allyl 2-propenethiosulfinate), isolated from garlic, is decomposed in aqueous acetone, an oily mixture of the *E* and *Z* isomers of ajoene results (Fig. 1). While many studies of the pharmacological effects of ajoene continued to use mixtures of the two isomers, more recent studies have also paid attention to establishing their individual properties. Thus, both (*E*)- and (*Z*)-ajoene were recently shown to possess antidiabetic activity [8] and hypocholesterolemic activity [7], and to lower the levels of uric acid in the blood [13], while (*E*)-ajoene was specifically used to control the fungus *Candida Albicans* at doses of 5 μg/mL [14] and (*Z*)-ajoene, as an experimental antileukemic, was very recently shown to induce apoptosis in human promyeloleukemic HL-60 cells [15].

Our interest in ajoene focuses on its possible complexation with cyclodextrins (CDs, cyclic oligosaccharides composed of D-glucopyranose units), which could result in the formation of inclusion complexes with potential medicinal applications [16]. We consider an approach in which well-defined, pharmacologically active garlic constituents are selected for inclusion to be more desirable than one using mixtures or whole extracts. In the present study, we underscore this approach by investigating the inclusion properties of the individual *E* and *Z* isomers of ajoene. A practical advantage to be gained

*Corresponding author. E-mail: xraymino@science.uct.ac.za

ISSN 1061-0278 print/ISSN 1029-0478 online © 2004 Taylor & Francis Ltd
DOI: 10.1080/10610270412331285996

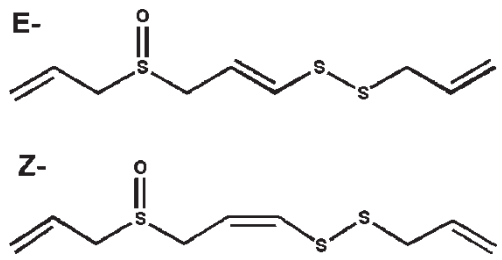

FIGURE 1 Chemical structures of the isomers of ajoene.

by CD inclusion complex formation in this instance is the conversion of these liquid guests into solids, rendering them more manageable for formulation. Production of stoichiometric inclusion complexes should further contribute to reproducible dosage formulations. Finally, the bioavailability of ajoene should be improved, as usually results when drugs are administered in the form of their CD inclusion complexes [16]. Previous use of CDs in relation to ajoene involved dissolution of its precursor allicin in water and/or a water-miscible solvent, and complexation of the allicin with α-, β- or γ-CD or a mixture of these. Further processing evidently led to subsequent formation of ajoene and its recovery by decomplexation and extraction of the dried complex [17].

Here we report the preparation of inclusion complexes formed between both (*E*)- and (*Z*)-ajoene and the host heptakis(2,3,6-tri-*O*-methyl)-β-CD (or TRIMEB), as well as the characterization of these complexes by thermal analysis, powder and single-crystal X-ray diffraction. TRIMEB was selected as a model host as the majority of our previous X-ray studies of TRIMEB-drug complexes successfully revealed ordered included guests (e.g. (*S*)-naproxen [18], (*S*)-ibuprofen [19], clofibric acid [20]), whereas guests included in the native CD hosts may be extensively disordered [21]. The lack of hydrogen-bond donors in both (*E*)- and (*Z*)-ajoene nevertheless suggested that only weak hydrophobic host–guest interactions should predominate. Coupled with the conformational flexibility of these guest molecules implied by their serpentine shapes, some degree of guest disorder was expected. At 173 K, molecular disorder is in fact manifested by the presence of both stereoisomers of (*E*)- and of (*Z*)-ajoene, in equal proportions, in their respective host CD molecules.

MATERIALS AND METHODS

Complex Preparation and Preliminary Characterization

TRIMEB was purchased from Cyclolab (Hungary) while (*E*)- and (*Z*)-ajoene were synthesized using the method of Block *et al.* [12]. TRIMEB (122 mg, 0.08 mmol) was dissolved in 0.61 mL of cold (± 2°C) distilled water in a vial. An equimolar amount (0.08 mmol) of (*E*)- or (*Z*)-ajoene was added with vigorous stirring. Precipitates formed immediately on addition of the respective guest isomers. Each vial was again cooled in an ice bath at (± 2°C) until the precipitate dissolved, but the solutions remained turbid. Stirring was continued overnight. The solutions were heated to 60°C for 12 h to induce crystallization. Several crystals of each complex were removed from the mother liquor, dried and prepared for thermal analyses. Water content was determined on fresh crystals by thermogravimetry (TGA). Complex crystals were examined by differential scanning calorimetry (DSC) on a Perkin Elmer PC7 system under N_2-purge (flow rate 30 mL/min). Samples (4–7 mg range) were scanned at 10 K/min over the range 30–300°C. Vented pans were used in DSC and the instrument was calibrated with high-purity indium and zinc standards. Hot-stage microscopy (HSM) was performed on a Linkam THMS600 apparatus with a Linkam TP92 manual temperature controller. All samples were covered with silicone oil to detect guest loss through the evolution of bubbles. A heating rate of 10 K/min was used. The host–guest ratio (1:1) in the complexes was determined in each case from UV spectrophotometric absorbance measurements recorded at 241 nm for **1** and 235 nm for **2** on a Cintra 20 UV system with the crystals dissolved in a water–ethanol solution (40:60 v/v).

Crystal Structure Analysis

Intensity data were collected on a Nonius Kappa CCD diffractometer from crystals coated with Paratone N oil (Exxon) and cooled using a Cryostream cooler (Oxford Cryosystems). Crystal systems and space groups were deduced from the Laue symmetries and systematic absences respectively. Data-collection (COLLECT software [22]) involved a combination of ϕ- and ω-scans of 0.7–1.0° for **1** and 1.0° for **2** with respective crystal to detector distances of 55 and 50 mm. Unit cell refinement and data reduction were performed with the program DENZO-SMN [23]. The structure of complex **1** was solved by Patterson search methods [24] using the rigid host moiety of the complex TRIMEB·(*S*)-naproxen [18] as a trial model. Isomorphous replacement with the same model was used to solve the phase problem for complex **2**. Guest atoms generally appeared with low electron densities due to disorder and were tediously located in a series of successive difference electron density maps. It became evident that each guest molecule was disordered over two positions, each corresponding to a stereoisomer of the respective guest (*E*)- or

(*Z*)-ajoene. Least-squares refinements of **1** and **2** were sensitive and several distance restraints were imposed on the individual components of the disordered guest molecules to ensure reasonable molecular geometries. All guest atoms were treated with a common isotropic temperature factor, which refined to 0.101(1) Å^2 for **1** and 0.146(1) Å^2 for **2**. The site-occupancy factors of the major stereoisomers in **1** and **2** refined to 0.51 and 0.54, respectively. Except for disordered methyl groups, host atoms were generally treated anisotropically and refined without restraints. The oxygen atom of the water molecule in **1** was located and assigned a site-occupancy factor (s.o.f.) of 0.5 on the basis of TGA data (see below) and its close proximity (*ca* 2.9 Å) to one of the disordered C atoms of a host methyl group. The latter group was located at two sites with equal electron densities, justifying assignment of 0.5 for the s.o.f.s of these components as well as that of the water O atom. Water H atoms could not be located. Host and guest H atoms were generally added in idealized positions in a riding model with $U_{iso} = 1.2$ times those of their parent atoms. Full-matrix least-squares refinement against F^2 (SHELXL97 [25]) was used with a weighting scheme $w = [\sigma^2(F_o^2) + (aP)^2 + bP]^{-1}$ and $P = [\max(F_o^2, 0) + 2F_c^2]/3$. Major residual electron density peaks in **2** were located within 0.10 Å of atom S4A and were attributed to its anisotropic motion. However, guest disorder did not warrant anisotropic refinement. The CIF files for the structures of **1** and **2** have been deposited with the Cambridge Crystallographic Data Centre (deposition numbers CCDC 229774 and 229775).

RESULTS AND DISCUSSION

Thermal Analysis

Figure 2 shows combined TGA and DSC traces for **1** and **2**. Complex **1** consistently showed a very small weight loss in the temperature range 30–60°C. This was interpreted as dehydration from HSM observation of bubble formation in this temperature range from crystals immersed in silicone oil. Measured weight losses were in the range 0.6–0.8% ($n = 3$), corresponding to about 0.5 water molecules per complex unit. Following dehydration, complex **1** melted at 143.8°C. Both HSM and DSC confirmed that complex **2** is unsolvated, showing only fusion at 140.5°C. (The very small, reproducible endotherm following fusion of **2** has onset temperature 144.8°C and is due to contamination by complex **1**, due to the presence of (*E*)-ajoene at a *ca* 5% level in the sample of (*Z*)-ajoene used for complex **2** preparation.) The complex melting points are sufficiently different from that of the pure host (157–159°C), and from one another, to be useful for complex identification. Following fusion, complexes **1** and **2** begin to decompose exothermically at onset temperatures of approximately 160°C.

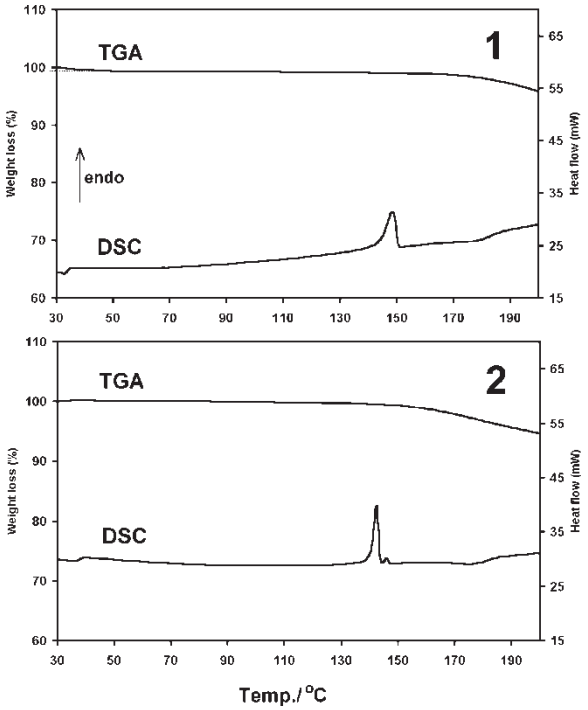

FIGURE 2 TGA and DSC traces for the complexes **1** and **2**.

X-ray Analysis

Overall Description of the Structures

Crystal data and details of the structural refinements are listed in Table I. The asymmetric unit for complex **1** comprises one TRIMEB molecule, half a molecule of each stereoisomer of (*E*)-ajoene, and half a molecule of water. Complex **2**, containing (*Z*)-ajoene, is analogous to **1** but is anhydrous. The host conformations are very similar in the two complexes, but the modes of guest inclusion are distinctly different, resulting in different crystal packing arrangements.

Structures and Conformations of the Guest Molecules

For the inclusion complex **1**, between TRIMEB and (*E*)-ajoene, Fig. 3 shows the peaks assigned (and refined) as non-hydrogen guest atoms in the composite electron density image A–B, together with the assigned atom connectivities, while the deconvoluted models are labelled A and B. It is evident that A and B share common terminal atoms C1, C2, C3 and S10, C11, C12, C13, with corresponding atoms being chemically equivalent.

TABLE I Crystal data and refinement details for the inclusion complexes **1** and **2**

Complex formula	$C_{63}H_{112}O_{35}\cdot(E)$—$C_9H_{14}OS_3\cdot 0.5H_2O$ (**1**)	$C_{63}H_{112}O_{35}\cdot(Z)$—$C_9H_{14}OS_3$ (**2**)
Formula weight	1672.92	1663.91
Temperature/K	173(2)	173(2)
Crystal system	Monoclinic	Orthorhombic
Space group	$P2_1$	$P2_12_12_1$
Unit cell dimensions		
a/Å	11.5531(2)	15.1019(2)
b/Å	27.715(1)	21.5196(3)
c/Å	14.6053(3)	27.313(1)
β/°	109.386(1)	–
Volume/Å^3	4411.4(2)	8876.4(4)
Z	2	4
Density (calculated)/g cm^{-3}	1.259	1.245
Radiation, wavelength/Å	Mo Kα, 0.71073	Mo Kα, 0.71073
Absorption coeff./mm^{-1}	0.167	0.166
F(000)	1798	3576
Crystal size/mm	0.53 × 0.40 × 0.25	0.35 × 0.34 × 0.31
Theta range/°	1.87–23.03	1.54–25.35
Index ranges	$-12 \le h \le 10$, $-29 \le k \le 30$, $-10 \le l \le 16$	$-17 \le h \le 17$, $-25 \le k \le 22$, $-21 \le l \le 32$
Reflections collected	10 160	31 007
Observed reflections [$I > 2\sigma(I)$]	7919	10 433
Data/restraints/parameters	8699/21/752	15252/27/950
Goodness-of-fit on F^2	1.051	1.017
Final R indices [$I > 2\sigma(I)$]	$R_1 = 0.0936$, $wR^2 = 0.2406$	$R_1 = 0.0906$, $wR^2 = 0.2321$
R indices (all data)	$R_1 = 0.1007$, $wR^2 = 0.2476$	$R_1 = 0.1344$, $wR^2 = 0.2657$
Largest diff. peak and hole/e Å^{-3}	−0.638, 0.659	−1.056, 1.172

However, the indicated connectivities necessitated by the twofold disorder of the sulfinyl group and atom S9 imply that in model A, C7–C8 is formally the central double bond (Fig. 1), while in model B this role is assumed by C8–C8B. The torsion angles around the respective C—C═C—S bonds are 163(2)° and 172(2)°, approximating the ideal value of 180° for the (*E*)-isomer. We note that the stereogenic sulfoxide sulfur atoms S4A and S4B have opposite configurations and hence the process of inclusion of (*E*)-ajoene has 'frozen out' the two stereoisomers, models A and B corresponding to the (*R*)- and (*S*)-enantiomers, respectively. The refined s.o.f.s indicate practically equal occupancy of these stereoisomers and therefore the TRIMEB molecule displays no stereorecognition

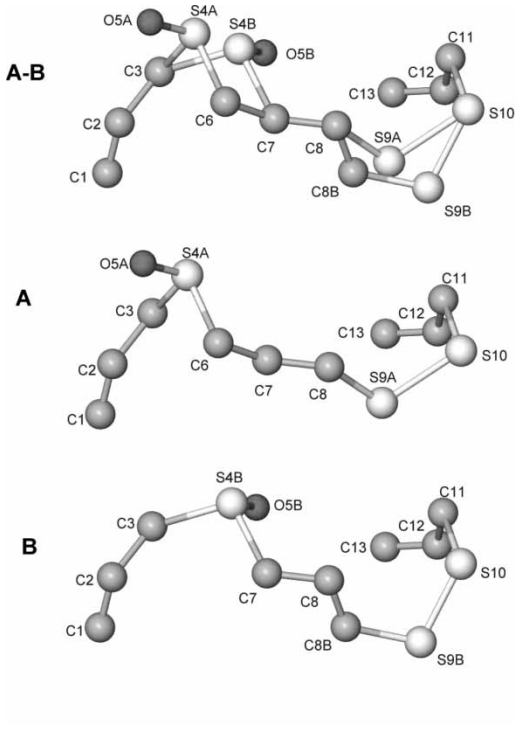

FIGURE 3 Disordered guest peaks in **1** (A–B) and the individual enantiomers (A = *R*-enantiomer, B = *S*-enantiomer) with atom assignments.

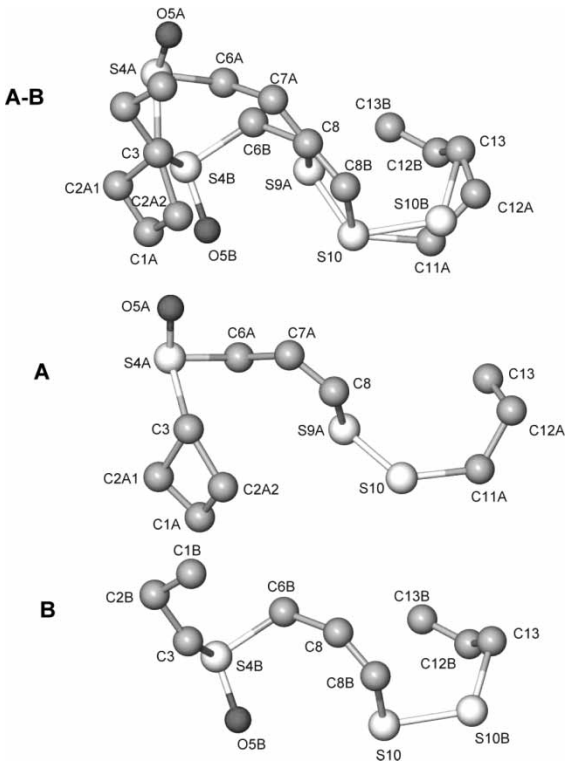

FIGURE 4 Disordered guest peaks in **2** (A–B) and the individual enantiomers (A = *R*-enantiomer, B = *S*-enantiomer) with atom assignments.

under the conditions of preparation viz. 1:1 host–guest ratio. The diastereomers TRIMEB–(A), TRIMEB–(B) therefore coexist in the crystal in a 1:1 molar ratio.

Figure 4 is the equivalent diagram describing guest disorder in the TRIMEB·(*Z*)-ajoene complex. This disorder is somewhat more complicated as only four atomic sites of the two disordered components A and B coincide, namely C3, C8, S10 and C13, all other atoms being disordered over two sites each. In component A, the central double bond is C7A–C8 while in component B it is C8–C8B. The C—C═C—S torsion angles are 16(3)° and 24(3)°, which approximate the ideal value of 0° for the *Z*-configuration of ajoene. Component A is further complicated in that atom C2 is disordered over two sites (C2A1, C2A2). Comparison of the stereochemistries of models A and B shows that again, the S atoms of the respective sulfoxide functions have opposite configurations and hence the process of inclusion of (*Z*)-ajoene in TRIMEB has likewise 'frozen out' its stereoisomers. Models A and B correspond to the (*R*)- and (*S*)-enantiomers of (*Z*)-ajoene respectively. As for (*E*)-ajoene, the TRIMEB molecule does not discriminate between the enantiomers of (*Z*)-ajoene, the refined s.o.f.s indicating their presence in almost equal proportions. The crystal thus also contains the two diastereomeric complex units in equal proportions.

Host Conformations and Modes of Guest Inclusion

As the structures were solved using a common TRIMEB skeleton as model, it was expected that the refined host conformations in **1** and **2** would be very similar. This was confirmed visually (Fig. 5) and from detailed comparison of the molecular parameters listed in Tables II and III. These include the glycosidic oxygen angle O4G($n-1$)$\cdots$O4G(n)$\cdots$O4G($n+1$), the radius of the heptagon (measured from the centroid of the seven O4 atoms to each O4 atom), the glycosidic O4G$n\cdots$O4G($n+1$) distance, the tilt angle of each glucose residue (defined in Table II) and the deviation of each O4 atom from the least-squares plane defined by all seven O4 atoms. There is generally a remarkable similarity between corresponding parameters for the host molecules in **1** and **2**. Their conformations are stabilized by several analogous intramolecular C—H$\cdots$O hydrogen bonds [18]. One notable difference relates to the tilt angles of the methylglucose residues. These parameters are sensitive to small perturbations at the secondary face, in this case the presence of the partial water molecule O1 in **1**. To accommodate its hydrogen-bond interactions with O3G5 and O2G4 [respective O1$\cdots$O distances 2.74(3) and 2.91(3) Å], residues G4 and G5 are significantly twisted towards (+11.5°), and away from (−4.1°), the host primary side respectively, relative to their orientations in complex **2**. All other corresponding residues in **1** and **2** have tilt angles differing by only ±2°. Other conformational differences noted are the opposite signs of the torsion angles O5—C5—C6—O6 in G4 [(−)-*gauche* in **1**, (+)-*gauche* in **2**], and again in G5, but with the reverse sign combination. The primary methoxyl groups of residues G2, G4, G5 and G7 are most effective in blocking the primary side of the host in both complexes. As shown by space-filling diagrams, the extent of closure is very similar despite the conformational differences described above. These complexes thus belong to the category of TRIMEB inclusion complexes in which the host cavity is cup-shaped [18,26], presenting a large hydrophobic surface to the encaged guest molecule.

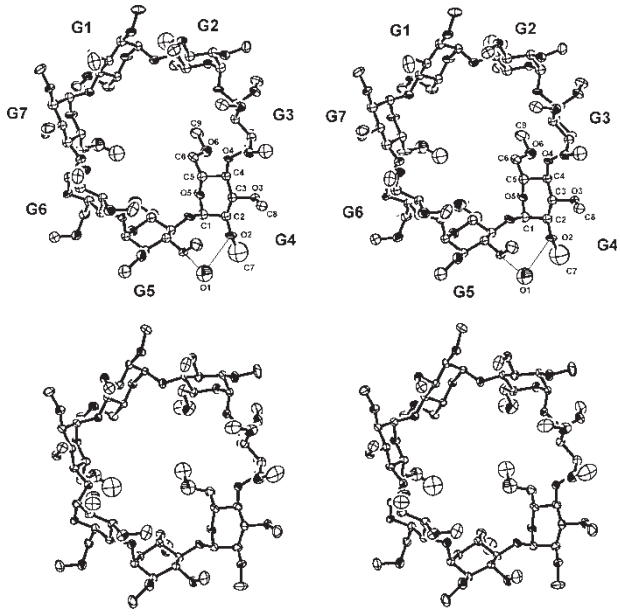

FIGURE 5 Stereoview of the host conformations in **1** (top) and **2** (bottom). For atoms refined anisotropically, thermal ellipsoids are drawn at the 40% probability level.

Modes of Guest Inclusion

As noted above, the resolved stereoisomers of (*E*)-ajoene overlap to a large extent (Fig. 2), which means that their overall modes of inclusion in TRIMEB are similar. These modes are compared in the stereoviews of Fig. 6, which show that in each case, the disulfide moiety is centrally placed and uppermost within the host cavity. The attached allylic and vinylic moieties are also included in the cavity, while the allyl group at the other terminus and its attached sulfinyl group protrude from the secondary face. The S═O dipole orientations are reversed for the two stereoisomers, and in one case (model A, *R*-enantiomer), there is a weak stabilizing

TABLE II Geometrical data for the host TRIMEB in complex **1**

(i) Glycosidic oxygen angle (°) and radius (Å) of the O4 heptagon measured from the centre of gravity of the seven O4 atoms to each O4 atom			
O4G7···O4G1···O4G2	123.8	G1	5.06
O4G1···O4G2···O4G3	128.5	G2	5.07
O4G2···O4G3···O4G4	123.0	G3	5.07
O4G3···O4G4···O4G5	138.0	G4	4.67
O4G4···O4G5···O4G6	118.5	G5	5.20
O4G5···O4G6···O4G7	124.9	G6	5.07
O4G6···O4G7···O4G1	134.6	G7	4.75
(ii) O4···O4′ distance/Å			
O4G1···O4G2	4.47	O4G5···O4G6	4.36
O4G2···O4G3	4.33	O4G6···O4G7	4.44
O4G3···O4G4	4.36	O4G7···O4G1	4.23
O4G4···O4G5	4.37		
(iii) Glucose residue number, value of tilt angle (°)[a], glycosidic O4 atom label and deviation (Å) of each O4 atom from the least-squares plane through the seven O4 atoms			
G1	14.3(3)	O4G1	−0.420(5)
G2	15.8(4)	O4G2	−0.164(5)
G3	9.8(4)	O4G3	0.404(5)
G4	54.3(4)	O4G4	0.113(5)
G5	32.0(2)	O4G5	−0.645(5)
G6	15.6(5)	O4G6	0.371(5)
G7	35.5(3)	O4G7	0.341(5)
			RMS deviation: 0.387

[a] Dihedral angle between the mean O4*n* plane ($n = 1$–7) and atoms O4G(n)–C1G(n)–C4G(n)–O4G($n + 1$).

interaction S═O···H—C(host) involving a secondary methyl group.

The modes of inclusion of the stereoisomers of (*Z*)-ajoene (Fig. 7) are distinctly different from those for the *E* isomer, as the disulfide group and its attached allyl group are now located outside the cavity and the sulfinyl group is within the cavity. There is, furthermore, a significant difference between the modes of inclusion of the individual stereoisomers of (*Z*)-ajoene, namely the location of their respective sulfinyl groups. Both are centrally located, but in A (*R*-enantiomer) the S═O group is situated at the 'roof' of the cavity, in van der Waals contact with the capping primary methoxyl groups, whereas in B (*S*-enantiomer) it is located near the secondary face. At location A, it engages in an S═O···HC(host methine) hydrogen bond.

Crystal Packing Arrangements and PXRD Patterns

As implied above, the complex units in **1** and **2** are topologically remarkably similar, except at the host secondary faces where chemically different

TABLE III Geometrical data for the host TRIMEB in complex **2**

(i) Glycosidic oxygen angle (°) and radius (Å) of the O4 heptagon measured from the centre of gravity of the seven O4 atoms to each O4 atom			
O4G7···O4G1···O4G2	127.8	G1	4.96
O4G1···O4G2···O4G3	125.4	G2	5.15
O4G2···O4G3···O4G4	124.0	G3	5.06
O4G3···O4G4···O4G5	136.7	G4	4.73
O4G4···O4G5···O4G6	121.0	G5	5.17
O4G5···O4G6···O4G7	125.6	G6	5.09
O4G6···O4G7···O4G1	131.5	G7	4.85
(ii) O4···O4′ distance/Å			
O4G1···O4G2	4.48	O4G5···O4G6	4.45
O4G2···O4G3	4.27	O4G6···O4G7	4.41
O4G3···O4G4	4.49	O4G7···O4G1	4.26
O4G4···O4G5	4.23		
(iii) Glucose residue number, value of tilt angle (°)[a], glycosidic O4 atom label and deviation (Å) of each O4 atom from the least-squares plane through the seven O4 atoms			
G1	13.7(1)	O4G1	0.407(3)
G2	15.8(2)	O4G2	0.240(3)
G3	11.7(1)	O4G3	−0.513(3)
G4	42.8(2)	O4G4	−0.023(3)
G5	36.1(2)	O4G5	0.556(3)
G6	13.5(2)	O4G6	−0.292(3)
G7	34.5(2)	O4G7	−0.375(3)
			RMS deviation: 0.382

[a] Dihedral angle between the mean O4*n* plane ($n = 1$–7) and atoms O4G(n)–C1G(n)–C4G(n)–O4G($n + 1$).

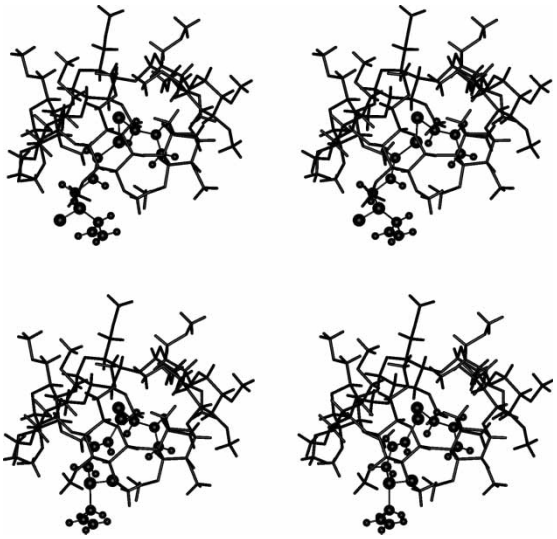

FIGURE 6 Stereoview showing the modes of inclusion of the enantiomers of (*E*)-ajoene in TRIMEB (*R*-enantiomer, top; *S*-enantiomer, bottom).

residues protrude. This difference induces distinctly different crystal packing arrangements, as initially inferred from the PXRD patterns (Fig. 8). The orthorhombic crystal system and space group $P2_12_12_1$ for complex **2** were initially deduced by finding a match between the experimental PXRD pattern and the reference pattern for a known isostructural series of TRIMEB complexes [27]. Although the experimental patterns for **1** and **2** have a superficial resemblance, detailed examination showed that the peak positions and relative intensities for **1** are unique [28]. (We recently reported what was evidently the first monoclinic crystal structure of a TRIMEB complex, that with the anaesthetic butamben as guest [29], also crystallizing in $P2_1$, but this has $a = 10.89$, $b = 14.86$, $c = 27.58$ Å, $\beta = 99.6°$ and is therefore not isostructural with complex **1**.) Each experimental PXRD is in very close agreement with its respective computed pattern.

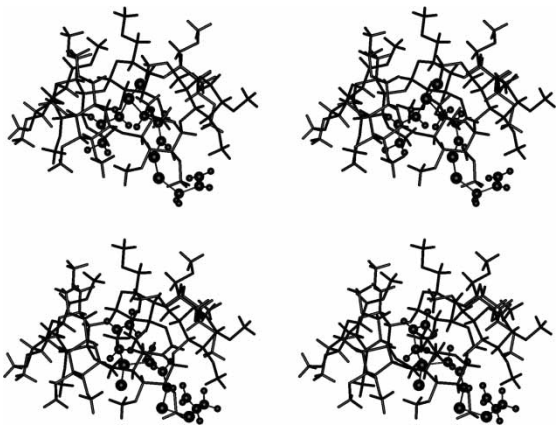

FIGURE 7 Stereoview showing the modes of inclusion of the enantiomers of (*Z*)-ajoene in TRIMEB (*R*-enantiomer, top; *S*-enantiomer, bottom).

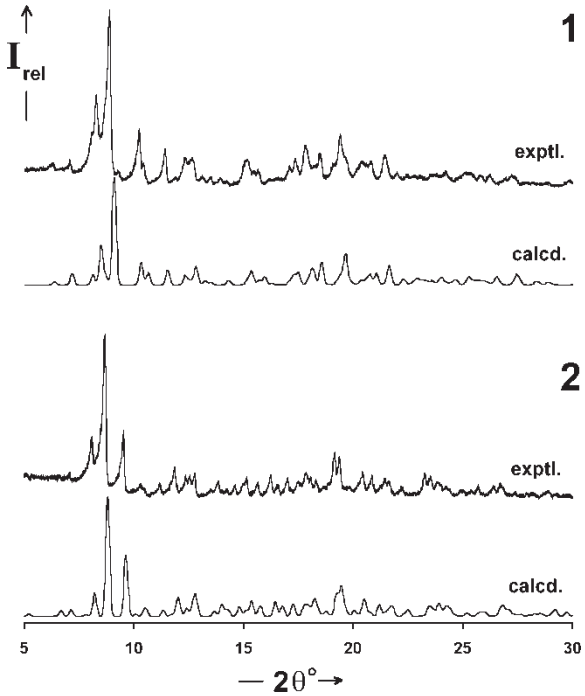

FIGURE 8 Experimental and computed PXRD traces for the complexes **1** and **2**.

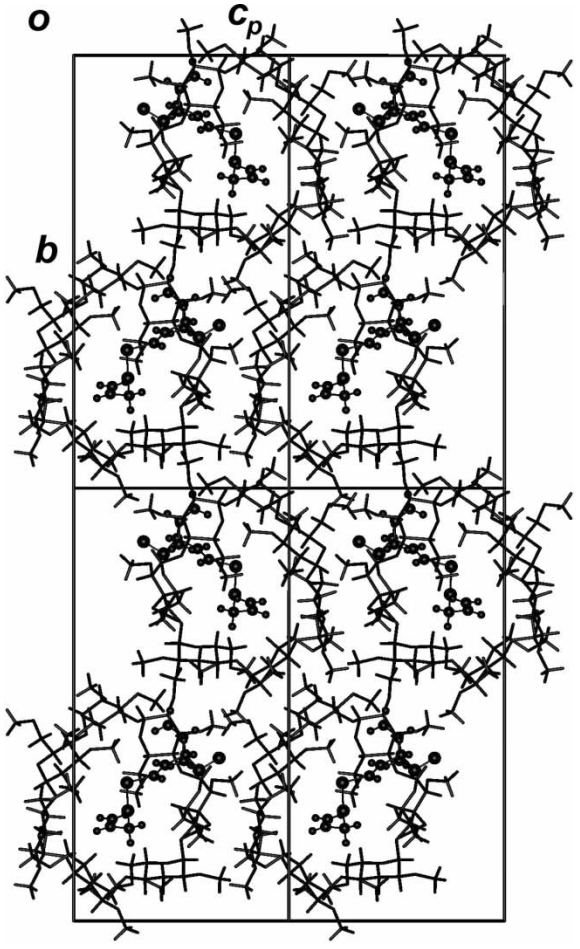

FIGURE 9 (100) Projection of the crystal packing in **1**.

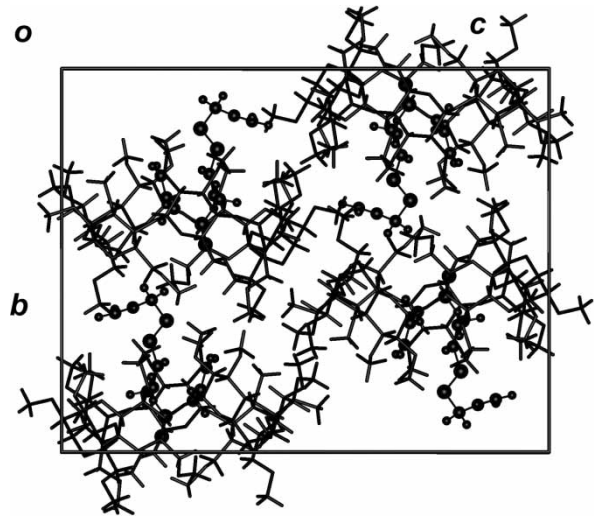

FIGURE 10 (100) Projection of the crystal packing in **2**.

Shifts to slightly higher 2θ angles in the calculated patterns are attributed to the different temperature conditions, namely 293 K (experimental) and 173 K (calculated).

The packing arrangements are shown in Figs. 9 and 10 with the (*R*)-enantiomer of each guest arbitrarily chosen for illustration. For **1**, the complex units are stacked in columns by translation along the *a* axis (~11.6 Å). The host O4 planes are parallel to (011) (i.e. steeply inclined to the *bc* plane) and the protruding guest residue is in contact with methoxyl groups of neighbouring host molecules. A single intermolecular hydrogen bond S═O···H—C(methylene)^{i} ($i = x, y, 1 + z$) for the guest (*R*)-enantiomer was identified. As the water molecule in **1** is hydrogen bonded to the host shown in Fig. 5, it cannot contribute to crystal stabilization by intermolecular hydrogen bonding. This was confirmed by the absence of short intermolecular O1···O contacts.

Complex **2** packs in the same well-known arrangement adopted by the TRIMEB inclusion complexes of (*S*)-naproxen [18] and (*S*)-ibuprofen [19]. The guest fragment protruding from the host secondary face is surrounded by methoxyl groups of neighbouring complex units and there are no intermolecular hydrogen bonds.

CONCLUSIONS

This study has shown conclusively that each of the isomers (*E*)- and (*Z*)-ajoene can be accommodated within a cyclodextrin host cavity to form thermally stable inclusion complexes **1** and **2**, respectively. X-ray analyses have confirmed the conformational flexibility of the ajoene isomers as well as the expected dominance of hydrophobic host-guest interactions in these complexes. In each complex, a disordered arrangement, comprising both the (*R*)- and (*S*)-guest enantiomers, was identified within the host cavity. X-ray refinement of site-occupancies also indicated that the TRIMEB molecule shows no stereo-discrimination under the conditions used for complex preparation. An interesting aspect of the study was the finding that in complex **2**, significantly different modes of inclusion are adopted by the individual guest stereoisomers. Finally, significant differences in the crystal packing of **1** and **2** are shown to be guest-induced, complex **1** crystallizing in a hitherto unknown arrangement for TRIMEB inclusion complexes. These results represent the first definitive thermal and structural data for cyclodextrin inclusion complexes of a major, pharmacologically active component from garlic. Further studies of the inclusion of related active compounds are in progress in this laboratory.

Acknowledgements

We thank the University of Cape Town and the NRF (Pretoria) for financial assistance. This material is based upon work supported by the National Research Foundation under Grant number NRF 2053361. Any opinions, findings and conclusions or recommendations expressed in the material are those of the author and do not necessarily reflect the views of the National Research Foundation.

References

[1] Agarwal, K. C. *Med. Res. Rev.* **1996**, *16*, 111.
[2] Qi, R.; Wang, Z. *Trends Pharmacol. Sci.* **2003**, *24*, 62.
[3] Apitz-Castro, R.; Cabrera, S.; Cruz, M. R.; Ledezma, E.; Jain, M. K. *Thromb. Res.* **1983**, *32*, 155.
[4] Whitmore, B. B.; Naidu, A. S. In *Natural Food Antimicrobial Systems*; Naidu, A. S., Ed.; CRC Press: Boca Raton, FL, 2000; p 349.
[5] Yoshida, S.; Kasuga, S.; Hayashi, N.; Ushiroguchi, T.; Matsuura, H.; Nakagawa, S. *Appl. Environ. Microbiol.* **1987**, *53*, 615.
[6] Baydoun, H.; Wagner, K.G.; Wagner, R.; Plank-Schumacher, K.; Scharfenberg, K.; Jain, M.K.; Apitz-Castro, R. Patent application DE 88-3821964 19880629, 1990.
[7] Hibi, K. Patent application JP 2000-18521 20000127, 2001.
[8] Hibi, K. Patent application JP 2000-122588 20000424, 2001.
[9] Tatarintsev, A.V.; Turgiev, A.S.; Davidson, J.B. Patent application US 96-585188 19960111, 1999.
[10] Walder, R.; Kalvatchev, Z.; Garzaro, D.; Barrios, M.; Apitz-Castro, R. *Biomed. Pharmacother.* **1997**, *51*, 397.
[11] Block, E.; Ahmad, S.; Jain, M. K.; Crecely, R. W.; Apitz-Castro, R.; Cruz, M. R. *J. Am. Chem. Soc.* **1984**, *106*, 8295.
[12] Block, E.; Ahmad, S.; Catalfamo, J. L.; Jain, M. K.; Apitz-Castro, R. *J. Am. Chem. Soc.* **1986**, *108*, 7045.
[13] Hibi, K. Patent application JP 2000-18522 20000127, 2001.
[14] Yoshida, S.; Nakagawa, S.; Gokuchi. T.; Matsura, H.; Uesugi, T. Patent application JP 86-105429 19860508, 1987.
[15] Min, L.; Min, J.-M.; Cui, J.-R.; Zhang, L.-H.; Wang, K.; Valette, A.; Davrinche, C.; Wright, M.; Leung-Tack, J. *Nutr. Cancer* **2002**, *42*, 241.
[16] Szejtli, J. *Chem. Rev.* **1998**, *98*, 1743.
[17] Dressnandt, G.; Rockinger, H.; Prigge, H.; Treiber, A. Patent application EP 96-100318 19960111, 1996.

[18] Caira, M. R.; Griffith, V. J.; Nassimbeni, L. R.; van Oudtshoorn, B. *J. Incl. Phenom. Mol. Recogn. Chem.* **1995**, *20*, 277.
[19] Brown, G. R.; Caira, M. R.; Nassimbeni, L. R.; van Oudtshoorn, B. *J. Incl. Phenom. Mol. Recogn. Chem.* **1996**, *26*, 281.
[20] Caira, M. R.; Bourne, S. A.; Mvula, E. N. *Biol. J. Armenia* **2001**, *53*, 148.
[21] Caira, M. R. *Roum. Chem. Q. Rev.* **2000**, *8*, 243.
[22] Hooft, R. *COLLECT*; Nonius, B.V. Delft, the Netherlands, 1998.
[23] Otwinowski, Z.; Minor, W. *Methods Enzymol.* **1997**, *276*, 307.
[24] Egert, E.; Sheldrick, G. M. *Acta Crystallogr.* **1985**, *A41*, 262.
[25] Sheldrick, G. M. *SHELXL97, Program for X-ray Crystal Structure Solution*; University of Göttingen: Germany, 1997.
[26] Harata, K. *Chem. Rev.* **1998**, 1803.
[27] Caira, M. R. *Rev. Roum. Chim.* **2001**, *46*, 371.
[28] *Cambridge Structural Database and Cambridge Structural Database System, Version 5.24*; Cambridge Crystallographic Data Centre, University Chemical Laboratory: Cambridge, UK, 2002.
[29] Caira, M.R.; Bourne, S.A.; Vilakazi, S.L.; Reddy, L. *Supramol. Chem*., **2004**, *16*, 279.